Neuron, Vol. 24, 739–750, November, 1999, Copyright ©1999 by Cell Press

Ataxia and Abnormal Cerebellar Microorganization in Mice with Ablated Contactin Gene Expression

Erik O. Berglund,* Keith K. Murai,*†
Barbara Fredette,* Gabriela Sekerková,‡
Beatrice Marturano,* Lynne Weber,*†
Enrico Mugnaini,‡ and Barbara Ranscht*†§
*The Burnham Institute
Neurobiology Program
La Jolla, California 92037
†University of California, San Diego
Department of Neuroscience
La Jolla, California 92093
‡Northwestern University
Institute for Neuroscience
Chicago, Illinois 60611

Summary

Axon guidance and target recognition depend on neuronal cell surface receptors that recognize and elicit selective growth cone responses to guidance cues in the environment. Contactin, a cell adhesion/recognition molecule of the immunoglobulin gene superfamily, regulates axon growth and fasciculation in vitro, but its role in vivo is unknown. To assess its function in the developing nervous system, we have ablated contactin gene expression in mice. Contactin$^{-/-}$ mutants displayed a severe ataxic phenotype consistent with defects in the cerebellum and survived only until postnatal day 18. Analysis of the contactin$^{-/-}$ mutant cerebellum revealed defects in granule cell axon guidance and in dendritic projections from granule and Golgi cells. These results demonstrate that contactin controls axonal and dendritic interactions of cerebellar interneurons and contributes to cerebellar microorganization.

Introduction

Developing neurons respond to an array of molecular signals that control the formation of axon trajectories and synaptic connections (Goodman and Shatz, 1993; Tessier-Lavigne and Goodman, 1996). Axon guidance and target recognition depend on interactions between neuronal cell surface receptors and cues in the extracellular environment that elicit selective growth cone responses. One class of molecules implicated in these processes is cell adhesion/recognition molecules of the immunoglobulin superfamily ([IgSF]; see Table 2 in Brümmendorf and Rathjen, 1995; Tessier-Lavigne and Goodman, 1996). Expression of IgSF cell adhesion molecules in association with subpopulations of extending axons in vivo (Walsh and Doherty, 1997), and demonstration of in vitro functions in modulating neurite growth (Rathjen and Jessell, 1991), suggest roles in the formation of axon projections in the developing nervous system. Indeed, recent work has revealed abnormal axon projections in mice with disrupted expression of IgSF cell adhesion molecule genes, including neural cell adhesion molecule ([NCAM]; Cremer et al., 1997; Seki and Rutishauser, 1998), L1 (Dahme et al., 1997; Cohen et al., 1998), and deleted in colon cancer ([DCC]; Fazeli et al., 1997).

Contactin, a neural IgSF cell adhesion/recognition molecule, delineates subpopulations of axons in the central and peripheral nervous system (Ranscht et al., 1984; Ranscht, 1988; Gennarini et al., 1989; Berglund et al., 1991; Hosoya et al., 1995; Yoshihara et al., 1995). Experiments in vitro implicate contactin in regulating neurite extension (Gennarini et al., 1991; Durbec et al., 1992), repulsion (Pesheva et al., 1993), and fasciculation (Chang et al., 1987; Rathjen et al., 1987; Buttiglione et al., 1996). Contactin is anchored in the cell membrane through a glycosylphosphatidyl inositol (GPI) moiety (Brümmendorf et al., 1989; Gennarini et al., 1989; Berglund and Ranscht, 1994) and can occur in a soluble form (Durbec et al., 1992). Therefore, it can potentially act both as a neuronal receptor and as a substrate for neurite growth. Contactin is thought to exert these multiple functions through interactions with different heterophilic ligands. Contactin's immunoglobulin-like and fibronectin type III (FNIII)-like domains provide binding sites for a variety of molecules, including other IgSF cell adhesion molecules (Brümmendorf et al., 1993; Morales et al., 1993; Sakurai et al., 1997; Buttiglione et al., 1998; Volkmer et al., 1998), tenascins (Rathjen et al., 1991; Zisch et al., 1992; Brümmendorf et al., 1993; Pesheva et al., 1993), receptor tyrosine phosphatase β (RPTPβ/phosphacan; Peles et al., 1995; Sakurai et al., 1997), and contactin-associated protein ([Caspr]; Peles et al., 1997). Despite the identification of these molecular interactions, the role of contactin in neural development remains unknown.

To gain an understanding of how contactin functions in the nervous system, we have generated mice with disrupted contactin gene expression by homologous recombination in embryonic stem cells. Ablation of contactin protein caused a severe ataxic phenotype consistent with cerebellar dysfunction (Pellegrino and Altman, 1979). Based on this phenotype, we focused the current analysis on the microorganization of the cerebellum. Our results demonstrate that contactin is necessary for organizing axonal and dendritic projections from cerebellar interneuron populations. This work thus identifies the vital role of the IgSF cell adhesion/recognition molecule contactin in cerebellar development in vivo.

Results

Contactin Expression in the Postnatal Mouse Cerebellar Cortex

The mouse cerebellum is an excellent system to study the role of contactin in establishing neuronal projections. Its anatomical organization and postnatal development are well characterized, and contactin is prominently expressed in the postnatal cerebellar cortex (Gennarini et

§To whom correspondence should be addressed (e-mail: ranscht@burnham-inst.org).

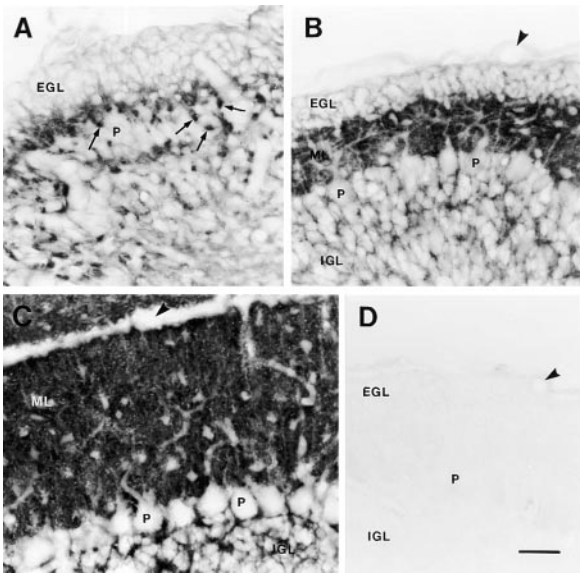

Figure 1. Contactin Expression in the Postnatal Mouse Cerebellum

(A) At P0, contactin is expressed throughout the external granule cell layer (EGL). Staining is most intense on postmitotic premigratory neurons and their early extending axons in the inner portion of the EGL (arrows). Purkinje cells (P) are negative.

(B) At P11, cells in the EGL remain positive for contactin immunohistochemistry. Staining is most intense in the molecular layer (ML) where the axons of granule cells extend and fasciculate. In the internal granule layer (IGL), staining is seen in clusters representing the glomeruli. Note the absence of contactin staining on epithelial cells of the pia mater (arrowhead in [B], [C], and [D]).

(C) At P15, contactin staining is abundant on parallel fibers in the ML and in glomeruli of the IGL. Purkinje cells and their dendritic arborizations remain negative for contactin staining throughout postnatal development.

(D) Staining of P11 cerebellum with preimmune serum is negative. Scale bar, 50 μm. All sections show sagittal view.

al., 1989; Faivre-Sarraihl et al., 1992). Contactin mRNA is synthesized by granule cells, the major cerebellar interneuron population localized in the internal granule layer (IGL) (Yoshihara et al., 1995). Granule cells project T-shaped axons, the parallel fibers, into the molecular layer (ML), and represent the major presynaptic afferent of Purkinje cells. Golgi cells, a population of large interneurons in the IGL, express contactin both on dendritic projections into the ML and on axon collaterals in the IGL (Faivre-Sarraihl et al., 1992). In the IGL, the terminal branches of each Golgi cell axon join into a synaptic complex, the glomerulus, with granule cell dendritic expansions and an afferent mossy fiber terminal (Palay and Chan-Palay, 1974).

In order to view the dynamic changes of contactin protein expression, we analyzed sections of the postnatal mouse cerebellum at postnatal day 0 (P0), P11, and P16 by immunohistochemistry with contactin antisera. Contactin was detected in the cerebellum throughout postnatal development, and its expression increased over time (Figure 1). At P0, contactin was distributed on granule cell bodies in the external granule layer (EGL) and was particularly enriched on the premigratory granule cells in the inner portion of the EGL. In the developing ML, contactin was expressed on early extending parallel fibers (Figure 1A). At P11 (Figure 1B), contactin immunostaining was maintained on granule cells in the EGL. In the ML, contactin expression increased on the parallel fibers, coincident with the organization of parallel fibers into fascicles (Figure 1B). Postmigratory granule cells that had settled into the IGL expressed contactin at low levels on their cell bodies. In the IGL, contactin was observed in clusters corresponding to the glomeruli.

By P16, when the ML was fully formed, contactin was strongly expressed on the parallel fibers and in the IGL (Figure 1C). The white matter tracts within the cerebellar folia contained contactin-positive afferent mossy and/or climbing fibers (data not shown). Purkinje cells and their processes were negative for contactin staining throughout postnatal development (Figure 1). No staining was obtained with the preimmune serum (shown at P11 in Figure 1D). Thus, contactin was expressed throughout postnatal cerebellar development and was concentrated on extending parallel fibers, in glomeruli, and on afferent mossy and/or climbing fibers.

Generation of Contactin Mutants

To investigate the in vivo role of contactin in mouse cerebellar development, mice with ablated contactin gene expression were generated by homologous recombination in embryonic stem (ES) cells. Contactin exon 3 (Buttiglione et al., 1995) was disrupted by insertion of a neomycin-resistance cassette (Figure 2A), and the mutation was transferred to ES cells. Germline chimeras were generated by injection of targeted ES cell clones into blastocysts. Mice homozygous for the contactin mutation were born at the expected frequency from heterozygous intercrosses. Genotypes were determined by Southern blot hybridization (Figure 2B) or by polymerase chain reaction (PCR).

Ablation of Contactin Protein Expression in Contactin Mutant Mice

Four independent lines of experimentation demonstrated that the mutation eliminated contactin protein expression. First, contactin was not detected in brain homogenates from mutant mice by Western blot analysis with any of four available contactin antisera (Figure 2C). Brain tissue from wild-type littermates contained abundant immunoreactive 135 kDa contactin protein (Figure 2C). Second, contactin protein was not apparent by immunohistochemistry on sections of mutant mouse cerebellum at P8 and P16 (data not shown). In contrast, contactin antibodies intensely stained the ML and clusters in the IGL of cerebellar sections from wild-type littermates (Figure 1). Third, cultured cerebellar granule cells from mutant mice did not show immunocytochemical staining for contactin, while neurons isolated from wild-type littermates displayed abundant contactin expression on neurites (data not shown). Finally, contactin was not detected in the pool of immunoprecipitated surface-biotinylated proteins from cultured mutant cerebellar granule cells. In contrast, the 135 kDa contactin protein was readily identified among the biotinylated surface proteins from wild-type cerebellar neurons (Figure 2D). Controls probing biotinylated proteins for L1, an IgSF cell surface adhesion molecule also expressed by cerebellar granule cells (Stallcup et al., 1985), showed

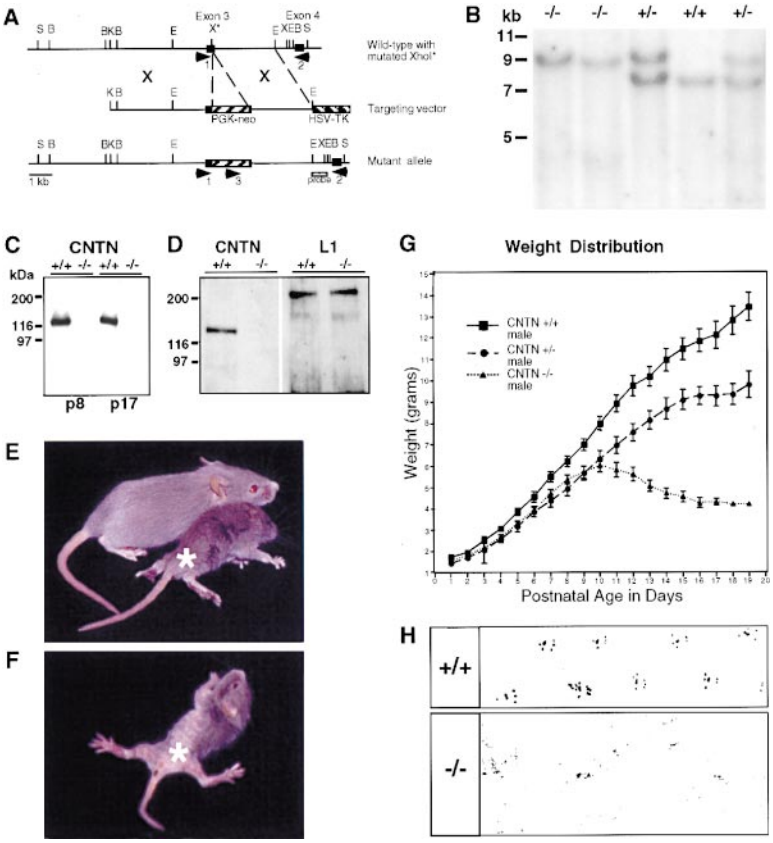

Figure 2. Figure 2. Disruption of Contactin Gene Expression in Mice

(A) Gene targeting vector. Contactin gene expression is disrupted by insertion of a PGK-neomycin cassette into exon 3. An HSV-TK cassette at the 3′ end of the targeting construct allows for negative selection in gangcyclovir.

(B) Genotyping. Southern blotting of BamH1-cut genomic DNA from litters of heterozygous intercrosses identifies the mutated 9 kb DNA fragment in contactin mutants (−/−) and the 7.4 kb DNA fragment in the wild-type animals (+/+). Heterozygous mutants (+/−) carry both the wild-type and the mutant allele. The probe is indicated in (A).

(C) Ablation of contactin protein in contactin mutant mice. Contactin, apparent by Western blotting as a 135 kDa protein in the cerebellum of P8 and P17 wild-type mice (+/+), is not detected in the mutant cerebellum (−/−).

(D) Absence of contactin protein from cultured mutant granule cells. Immunoprecipitation of cell surface-biotinylated proteins from cultured cerebellar granule cells detects contactin protein (CNTN) on the surface of wild-type (+/+) but not of contactin (−/−) mutant neurons. L1 used as a control is present in similar amounts on granule cell surfaces from both genotypes.

(E) Phenotype. Contactin mutant mice (asterisk) are easily recognized by their smaller sizes and emaciated appearance at P15. The mutant is shown next to a wild-type littermate.

(F) Ataxia. The ataxic behavior of the mutants (asterisk) results in frequent falls, from which the mice gain the upright position only with great difficulty.

(G) Body weight. Contactin mutant mice do not gain weight after P10. The diagram compares the body weight of males with wild-type ($CNTN^{+/+}$), heterozygous ($CNTN^{+/-}$), and homozygous contactin mutant ($CNTN^{-/-}$) genotype over postnatal development (n = 5). Contactin mutant mice die by P18, except when hand fed.

(H) Ataxic gait. Ink footprinting illustrates the broad-based gait and the dragging of the hindlimbs of contactin mutants (−/−).

similar amounts of this protein in neuronal immunoprecipitates from both genotypes (Figure 2D). These collective results demonstrate that the mutation had efficiently disrupted contactin protein expression in homozygous mutants.

Ataxic Phenotype and Early Postnatal Death of Contactin Mutant Mice

At birth, contactin mutants were indistinguishable from wild-type littermates. By P10, the mutants exhibited an overt ataxic phenotype that increased in severity over subsequent days. The defects in controlling voluntary movements, posture, and balance were accompanied by the failure to gain body weight and progressive weakening (Figure 2G). By P15, the homozygous mutants in a litter could be identified by their smaller sizes, emaciated appearance, and uncontrolled movements (Figures 2E and 2F). The mutation was lethal by P18.

The ataxic phenotype of mutants consisted of crawling forward as illustrated by hindfoot print patterns at P15 (Figure 2H). Their uncontrolled movements resulted in frequent falls and rollovers from which the mutants regained the upright position only with extreme difficulty (Figure 2F). In contrast to wild-type littermates, P15 mutants were unable to perform complex motor tasks, such as traversing an elevated 1 inch by 12 inch beam or climbing up a 30 cm long knotted rope. Gross vestibular functions appeared unimpaired as the mutants showed appropriate behavioral responses in tests for negative geotaxis and body positioning in water (Lim et al., 1978). Thus, the mutant mice displayed an overt ataxic phenotype that resembled that of mutants with localized cerebellar defects (The Mouse Genome Informatics, Jackson Laboratory [www.informatics.jax.org]; Sidman, 1968; Heintz et al., 1993).

Overall Cerebellar Organization in Contactin Mutant Mice

The gross anatomical organization of the cerebellum was examined in brain sections of P15 wild-type and mutant mice by Nissl stain. No remarkable differences between genotypes were noted in folia development or laminar organization. The mutant cerebellum, however, was smaller than that of wild-type littermates. To determine the extent of this size reduction, areas occupied by midsagittal cerebellar sections from wild-type and mutant mice were measured. At P15, cerebellar size of the mutants was reduced by 17.47 percent (5.00 ± 0.11 mm^2 [mean ± SEM] in the wild-type versus 4.13 ± 0.10

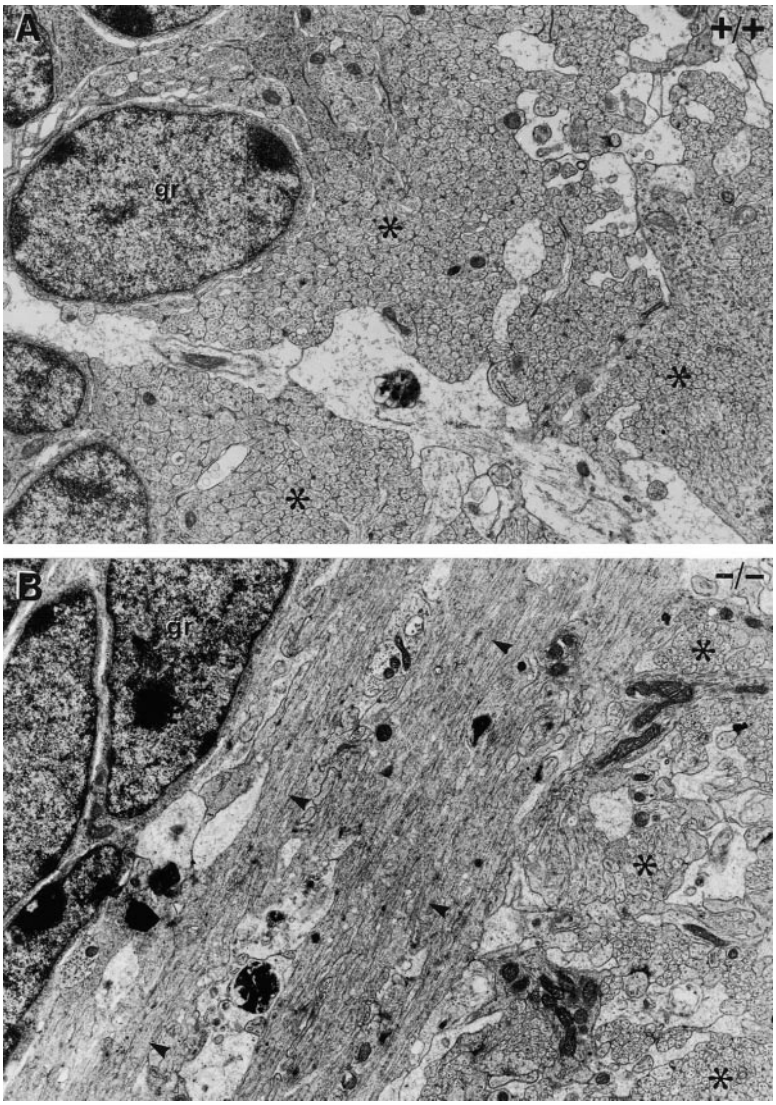

Figure 3. Misoriented Parallel Fibers in the Outer Cerebellar Molecular Layer of Contactin Mutants

(A) Parallel fibers in wild-type mice (+/+) are oriented perpendicular to Purkinje cell dendrites throughout the ML in sagittal view at P15.

(B) In contactin mutants (−/−), parallel fibers in the outer ML are misoriented (arrowheads) and project 90 degrees to parallel fibers in the inner and middle ML. Correctly oriented fibers are indicated by asterisks. Gr, granule cell in the EGL. Magnification, 5.5 K.

mm^2 [mean ± SEM] in mutant mice; significant at $p < 0.001$, unpaired two-tailed t test).

Misoriented Parallel Fibers in Contactin Mutant Mice

As granule cells are the major neuron population expressing contactin in wild-type mice (Figure 1), we performed detailed comparisons of granule cell organization and morphology in wild-type and mutant cerebella at P15-P16. Tracing of individual granule cells with DiI (Molecular Probes) and Golgi silver impregnation (Spacek, 1989) revealed the characteristic T-shaped branching of granule cell axons within the ML in both genotypes. As these techniques only detect individual fibers, the overall organization of parallel fibers was examined by electron microscopy. A dramatic defect was discovered in the orientation of the parallel fiber population in the outer portion of the ML in sagittal cerebellar sections from P15 mutant mice (Figure 3, $n = 3$ littermate pairs). In wild-type mice, parallel fibers were correctly oriented perpendicular to the plane of Purkinje cell dendrites within the entire ML (Figure 3A). In contrast, in contactin mutants, parallel fibers in the outer portion of the ML projected parallel instead of perpendicular to the plane of Purkinje cell dendritic branches (Figure 3B). This late developing population of granule cells thus extended axons at right angles to appropriately oriented parallel fiber populations within the inner portion of the ML. Ablation of contactin gene function had therefore resulted in the misguidance of granule cell axon subpopulations.

Fasciculation of Parallel Fibers in Contactin Mutant Mice

Contactin's reported role in mediating neurite growth and fasciculation in vitro (Chang et al., 1987; Rathjen et al., 1987; Buttiglione et al., 1996) prompted us to investigate neurite growth properties of mutant cerebellar granule cells in culture. Granule cells were obtained from P5-P6 wild-type and mutant cerebella and grown separately as reaggregate cultures (Gao et al., 1995). Granule cell clusters extended neurites independent of contactin gene expression. However, neurite growth

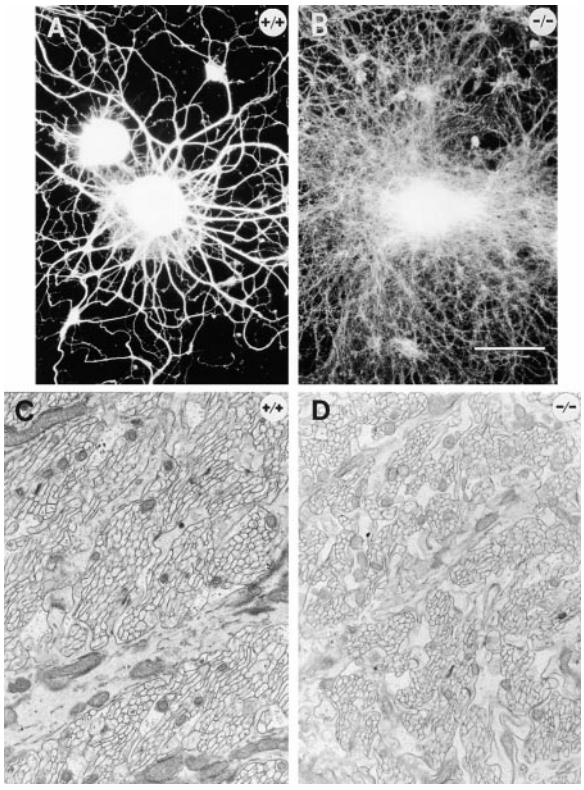

Figure 4. Fasciculation of Granule Cell Axons In Vitro and In Vivo

(A) Fasciculated neurite bundles extend from wild-type granule cell aggregates in culture.

(B) Neurites from contactin mutant granule cell clusters extend individually and are diffusely arranged.

(C and D) Electron micrographs of cross-sectioned parallel fibers in the ML of wild-type (C) and contactin mutant (D) cerebellum at P15 reveal fascicles in both genotypes. Measurements of the areas occupied by parallel fibers (see text) identify a small but significant increase in the spacing between axons in contactin mutants. Scale bar for (A) and (B), 100 μm. Magnification for (C) and (D), 21 K.

patterns differed dramatically between genotypes (Figure 4; n = 6 littermate pairs). Wild-type granule cell neurites were largely organized into fascicles (Figure 4A). In contrast, predominantly single neurites emerged from contactin-deficient granule cell aggregates producing a halo of fibers around cell clusters (Figure 4B). Defasciculated neurites were also observed when wild-type granule neurons were treated with antibodies to contactin but not in controls treated with normal IgG (data not shown). These results support the notion that contactin mediates neurite–neurite interactions in vitro that commonly serve as a paradigm for parallel fiber fasciculation in vivo.

To determine if this in vitro fasciculation defect applied to parallel fiber organization in vivo, the ML of wild-type and mutant cerebella was analyzed in cross-section by electron microscopy. Parallel fiber fascicles ensheathed by glial cell processes were observed in both genotypes, suggesting that the formation of fascicles and their astrocytic ensheathment occurred independent of contactin gene expression. However, a slight reduction in the compaction of parallel fibers within fascicles was noted in the mutant mice. Standard electron microscopy was used to determine the degree of compaction within fascicles. Axon density per unit area was assessed at P15 in three mutant and wild-type littermate pairs by measuring axon areas within fascicles and the spaces between them. Measurements were expressed as the percentage of axon area occupying the total fascicle region and provided a measure of parallel fiber proximity, or degree of fasciculation. Parallel fibers of wild-type mice occupied 76.5% ± 0.77 (mean ± SEM) of the total fascicle area, while the mutant axons occupied less, 72.7% ± 0.74 (mean ± SEM). This 3.8 percent difference, albeit small, was significant ($p < 0.0007$ by unpaired, 2-tailed t test). These data demonstrate that the formation of parallel fiber fascicle occurs independent of contactin gene expression. Contactin, however, appears to partake in the compaction of axons within fascicles and contribute to fascicle tightness.

Impaired Granule Cell Dendritic Expansions in Contactin Mutant Mice

The dendrites of granule cells in the IGL extend claw-like terminal branches that receive synaptic input from mossy fibers and Golgi cell axon terminals in the glomeruli (Hámori and Szentágothai, 1966; Mugnaini, 1972; Palay and Chan-Palay, 1974). To address if contactin-mediated interactions are necessary for the extension of granule cell dendrites, individual granule cells were labeled with DiI injected into the ML of P15 wild-type and mutant mice. Granule cell dendrites extended in both mutant and wild-type cerebella. In the wild-type, dendrites developed characteristic claw-like expansions at their terminals (Figure 5A). In contrast, the distal dendritic branches of mutant granule cells were stubby and underdeveloped (Figure 5B). To quantitate this difference, the areas occupied by the distal dendritic claws of DiI-labeled granule cells were measured and subjected to morphometric analysis. In wild-type mice, the mean distal dendritic area occupied 12.24 ± 0.51 μm^2 while the corresponding area covered 7.83 ± 0.38 μm^2 (mean ± SEM) in the mutants (n = 180 wild-type cells, and n = 182 mutant cells from three littermate pairs). This represents a 36% reduction of the distal granule cell dendritic surface area in contactin mutants (significant at $p < 0.001$, unpaired t test; Figure 5C). This decrease corresponds to a significant reduction of the granule cell postsynaptic area available for the formation of mossy fiber and Golgi cell synapses.

Aberrant Golgi Cell Dendrites in Contactin Mutant Mice

Golgi cells situated in the IGL express contactin on both axons and dendrites (Faivre-Sarrailh et al., 1992). To determine if ablation of contactin gene expression had affected these neurons, Golgi cells and their projections were monitored by mGluR2/3 staining (metabotropic glutamate receptor 2/3; Neki et al., 1996). In wild-type mice at both P13 and P17, Golgi cells projected branched dendrites into the ML (Figure 6A). In contrast, substantially fewer mGluR2/3-positive dendrites were detected in contactin mutants. The few dendrites that reached into the ML in the mutant cerebellum were stunted and showed little branching (Figure 6B). Staining for mGluR2/3 was comparable on Golgi cell bodies in

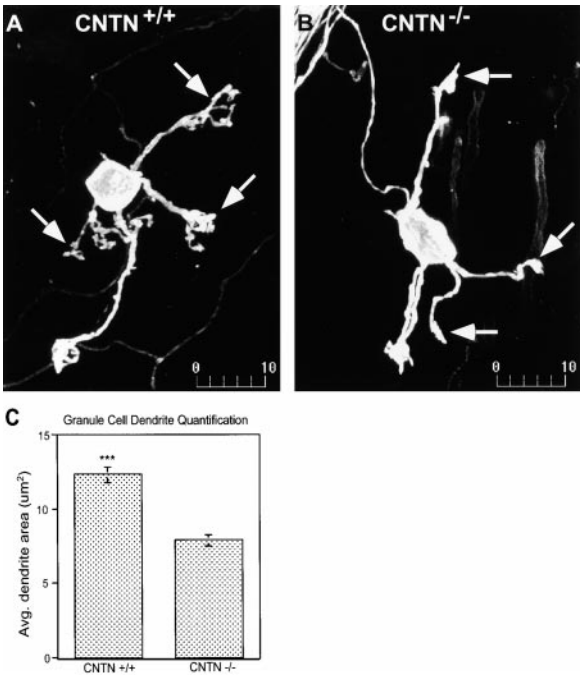

Figure 5. Reduction of Granule Cell Dendritic Expansions in Contactin Mutants

(A) DiI-labeled wild-type granule cells extend claw-like expansions at the distal ends of their dendrites at P16.

(B) Digitiform expansions of granule cell dendrites are stunted in contactin mutant littermates.

(C) Morphometric analysis of the areas occupied by the DiI-labeled terminal digitiform granule cell dendritic branches reveals a 36% reduction of the dendritic surface area in contactin mutants ($p < 0.0001$ by unpaired 2-tailed t test). Scale bar, 10 μm.

the IGL in both genotypes, indicating that the mutation had not overtly affected mGluR2/3 expression. Independent evidence for aberrant Golgi cell dendritic projections in contactin mutants was obtained by immunostaining for the cytoskeletal dendritic marker protein microtubule-associated protein-2 (MAP-2) (Figures 6D and 6E).

For quantitation, mGluR2/3-positive Golgi cell dendritic stalks traversing from the IGL into the ML were counted in P17 mutant and wild-type cerebellar sections and related to the per unit length of the cerebellar Purkinje cell layer. In the mutants, the number of mGluR2/3-positive Golgi cell dendrites extending through the Purkinje cell layer into the ML was reduced by 50% as compared to the wild-type (0.0275 ± 0.0018 fibers/μm Purkinje cell layer (mean ± SEM) in the wild-type versus 0.0138 ± 0.0017 fibers/μm Purkinje cell layer (mean ± SEM) in the mutants; significant at $p < 0.0001$, unpaired 2-tailed t test) (Figure 6C). These results suggest that contactin-mediated interactions are required for the extension of Golgi cell dendrites into the ML.

Purkinje Cells Display Abnormal Axonal Varicosities in Contactin Mutant Mice

Several studies have established that Purkinje cell development and function critically depend on signals from afferent fibers (Alvarado-Mallart and Sotelo, 1982; Cohen-Cory et al., 1991; Baptista et al., 1994). Although

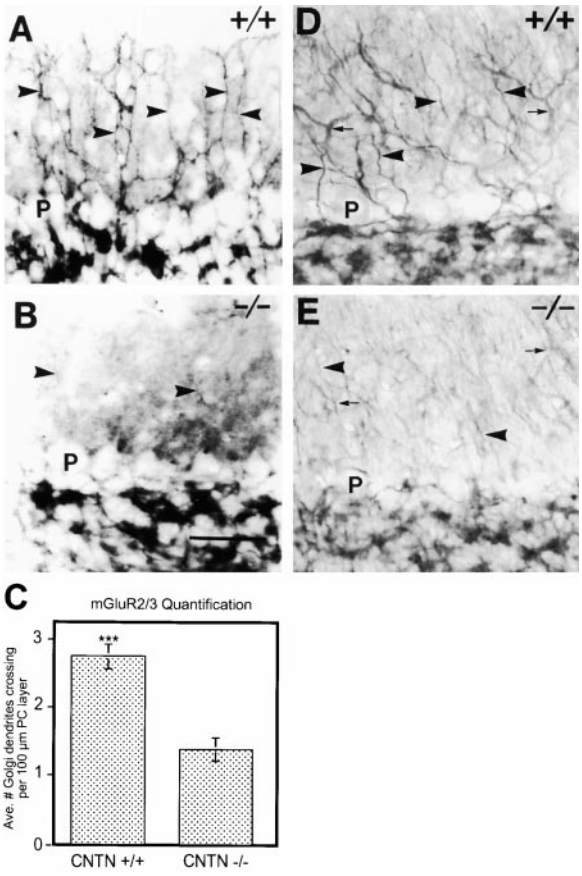

Figure 6. Reduction of Golgi Cell Dendritic Projections in Contactin Mutant Mice

(A) Golgi cell dendrites identified by staining for mGluR2/3 are branched and oriented radially into the ML of wild-type mice at P16.

(B) In mutants, Golgi cell dendrite projections into the ML are sparse, and the few extending dendrites are often stunted (arrowheads).

(C) Quantification of the number of Golgi cell dendrites extending from the IGL across Purkinje cell bodies into the ML. In mutants, 50% fewer dendrites project into the ML in comparison to wild-type mice ($p < 0.0001$ by unpaired 2-tailed t-test).

(D) Dendrites extending from the IGL across the Purkinje cell layer (arrowheads) and thick Purkinje cell dendrites (small arrows) are detected by MAP-2 staining in wild-type mice.

(E) In contactin mutants, few MAP-2-positive dendrites (arrowheads) extend from the IGL into the ML consistent with reduced Golgi cell dendritic projections. Scale bar, 50 μm.

Purkinje cells do not express contactin in wild-type mice, their development may be affected in contactin mutants through absence of contactin-mediated interactions with contacting cells. To explore this possibility, the morphology of Purkinje cells was monitored by DiI labeling and immunohistochemistry for calbindin-D28. DiI tracing of individual Purkinje cells at P15 and P16 revealed no remarkable differences between genotypes in their gross organization or overall dendritic branching (Figures 7A and 7B; $n = 5$ littermate pairs). Moreover, in both mutant and wild-type mice, Purkinje cell dendrites were studded with spines (Figures 7C and 7D). Consistent with this result, labeling of Purkinje cells with calbindin-D28 antibodies did not detect differences between genotypes in the number or positioning of Purkinje cell

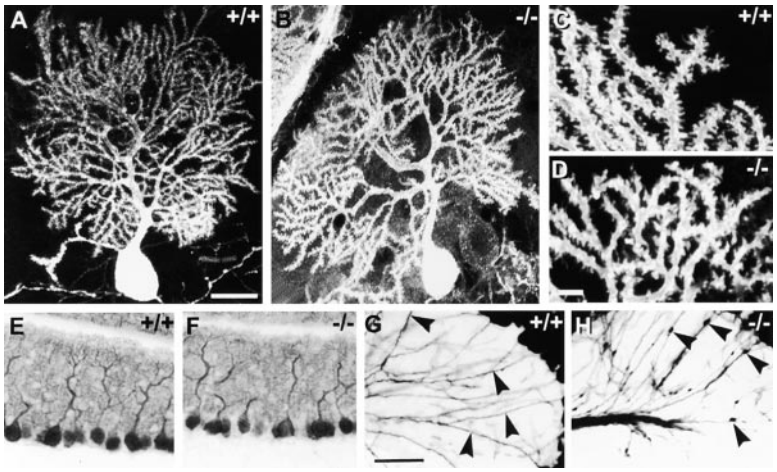

Figure 7. Purkinje Cell Development in Contactin Mutant Cerebellum

(A and B) DiI labeling shows comparable Purkinje cell dendritic morphology in wild-type and mutant cerebellum. Scale bar, 25 μm.

(C and D) Purkinje cell dendrites are studded with spines in both genotypes. Scale bar, 5 μm.

(E and F) Labeling for Calbindin-D28 shows the positioning of Purkinje cells in a single layer in both genotypes.

(G and H) At P15, calbindin-D28-positive Purkinje cell axons in mutants display abnormal swellings (arrowheads in [H]) that are not detected in wild-type littermates (arrowheads in [G]). Scale bar, 50 μm.

bodies or the organization of major dendritic arbors at P13, P15, and P17 (shown at P17 in Figures 7E and 7F).

Although no overt defects were noted in dendritic development, Purkinje cells in mutant mice displayed abnormal axon morphology. Immunostaining for calbindin-D28 detected axonal varicosities in the mutants that were not evident in wild-type littermates (Figures 7G and 7H). Such swellings frequently occurred in P13 mutants but were rarely observed at this age in the wild-type (data not shown). At P16, axon swellings persisted in mutants (Figure 7H, arrowheads), while axons of wild-type littermates were smooth (Figure 7G). This finding provides an indication for compromised Purkinje cell maturation or function in contactin mutant mice.

Discussion

This study provides in vivo evidence for the role of contactin in organizing neuronal projections. In accord with the abundant expression of contactin during postnatal cerebellar development, ablation of contactin gene expression causes a severe ataxic phenotype that is indicative of cerebellar dysfunction. In the present paper, we demonstrate that contactin plays a critical role in cerebellar microorganization. Ataxia caused by impaired cerebellar functions may interfere with normal feeding behavior and thus lead to the early postnatal death of contactin mutant mice. However, the defects identified in the current study may not fully explain the lethality of the mutation. Contactin expression on neurons integrated into other circuitries, such as the hypothalamo-neurohypophysial system (Pierre et al., 1998), may be vital for survival.

Contactin in Parallel Fiber Axon Guidance

During development, granule cell precursors in the EGL differentiate in an inside-out pattern, such that cells in the inner portion of the EGL extend axons before cells in the outer layers (Altman and Bayer, 1997). Granule cell axons extend parallel to the longitudinal axis of the folia and form beams of parallel fibers that are oriented perpendicular to the dendritic arborizations of Purkinje cells (Palay and Chan-Palay, 1974). In the mutants, the superficial parallel fibers abnormally project at a 90° angle relative to those deeper in the ML. The unique misorientation of mutant parallel fibers in only the outer portion of the ML suggests that early and late extending granule cell axons use different guidance mechanisms. Our analyses indicate that early differentiating granule cells in the EGL orient their axons independently of contactin, while the later developing neurons require contactin to achieve their correct perpendicular alignment. Little is known about the molecular mechanisms underlying bipolar alignment and directional axon extension of granule cells, except that cues provided by cells within the EGL are involved (Altman and Bayer, 1997). The current study has identified contactin as one of the molecular cues controlling parallel fiber orientation. Understanding of contactin-mediated interactions in this process will begin to further unravel the molecular bases of parallel fiber organization.

Contactin in the Fasciculation of Granule Cell Axons

A role for contactin in axon fasciculation was predicted from earlier in vitro studies that analyzed neurite growth on contactin substrates or in the presence of function-blocking antibodies (Chang et al., 1987; Rathjen et al., 1987; Buttiglione et al., 1996). We have used the mutant mice to clarify contactin's role in granule cell axon fasciculation. In accordance with previous reports, fasciculation of neurites from contactin-deficient cerebellar granule cells was severely disrupted in culture. Surprisingly, however, this defect was not recapitulated in vivo, as parallel fibers were fasciculated in the mutant mice. This discrepancy between in vitro and in vivo results may be explained by restrictions imposed in vivo on parallel fiber bundles by ensheathing glial cells. This restriction is removed when granule cells are grown as reaggregate cultures, allowing robust detection of compromised neurite–neurite interactions. This interpretation is compatible with the four percent decrease in compaction of mutant parallel fibers in situ. Taken together, these data demonstrate that contactin does not control the gross organization of parallel fiber fascicles in situ but appears to contribute to the compaction of axons and the tightness of parallel fiber fascicles.

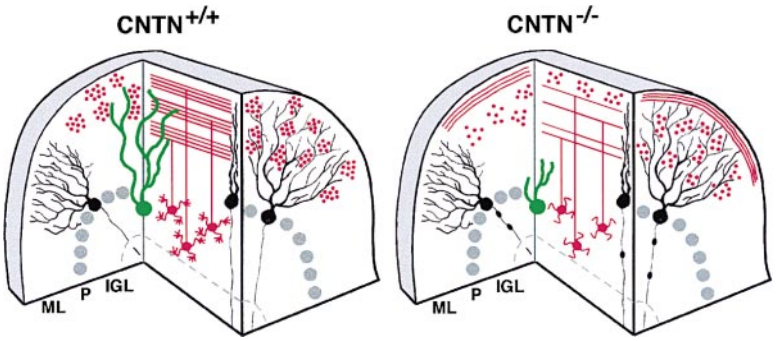

Figure 8. Role of Contactin in Cerebellar Microorganization

Contactin on granule cells (red) guides parallel fibers in the outer ML into their correct perpendicular orientation and supports the expansion of distal granule cell dendritic claws. Contactin also aids the compaction of granule cell axons, the parallel fibers, into fascicles. Golgi cells (green) require contactin to extend dendrites into the ML. Abnormal axonal varicosities in the mutants indicate compromised Purkinje cell function possibly through the absence of contactin-mediated interactions. Left, wild-type ($CNTN^{+/+}$); right, contactin mutant ($CNTN^{-/-}$).

Contactin in Granule and Golgi Cell Dendritic Development

Ablation of contactin gene expression impaired the expansion of distal granule cell dendritic claws and caused a significant reduction of granule cell postsynaptic area. Two interpretations may account for this result. First, contactin on granule cell dendrites functions as a neuronal receptor to interact with cues in the IGL for elaboration of the distal claws. However, this interpretation is unlikely given the fact that contactin has not been identified on granule cell dendrites (Faivre-Sarrailh et al., 1992). Alternatively, contactin localized to afferent Golgi and mossy fiber axon terminals (Faivre-Sarrailh et al., 1992) may promote interactions with granule cell dendrites during synaptogenesis. Thus, ablation of contactin gene expression may adversely affect adhesive interactions necessary for the formation of stable synaptic complexes within glomeruli and influence the morphology of the granule cell postsynaptic surface area.

Defective Golgi cell development indicated by aberrant dendritic projections may also contribute to the phenotype of contactin mutant mice. As both Golgi cells and parallel fibers in the ML express contactin in wild-type mice, either contactin on Golgi cell dendrites enables recognition of cues in the ML, or contactin on parallel fibers serves as an extracellular cue for the elaboration of Golgi cell dendrites. It is also possible that altered Golgi cell dendritic projections are secondary to compromised interactions in the glomeruli. Initial electron microscopic studies have revealed mossy fiber-granule cell synapses in the IGL; however, Golgi-granule cell contacts were hard to find (G. S. et al., unpublished data). More detailed investigations are necessary to clarify the underlying cause of the observed Golgi cell defect.

Ablation of Contactin Gene Expression Affects Purkinje Cells

Overall activity from extrinsic and intrinsic cerebellar neurons converges on Purkinje cells, which provide an integrated efferent from the cerebellar cortex. Although Purkinje cells do not express contactin, they receive inputs from several contactin-positive afferents, the majority of which are parallel fibers. Several studies have demonstrated that interactions with contacting cell populations, in particular granule cells, are crucial for Purkinje cell maturation (Alvarado-Mallart and Sotelo, 1982; Cohen-Cory et al., 1991; Baptista et al., 1994). Although Purkinje cells in the mutants showed no major impairments in overall dendritic morphology, they displayed abnormal axonal varicosities. Transient Purkinje cell axonal swellings were observed up to P14 in one study (Bäurle and Grüsser-Cornehls, 1994), and their continued presence in contactin mutants beyond this time may indicate abnormal Purkinje cell maturation. It is possible that contactin, which is concentrated on the distal ends of parallel fibers, including the presynaptic axon terminals (Faivre-Sarraihl et al., 1992), provides a direct signal to influence the maturation of Purkinje cells. However, this suggestion is unlikely since factors that influence Purkinje cell maturation generally correlate with abnormal dendritic morphology. An alternative interpretation is that Purkinje cells are affected through altered activity of parallel fibers. As discussed below, the misorientation and increased spacing between individual parallel fibers may compromise cross-talk between parallel fiber arrays and affect granule cell input onto Purkinje cells (Cohen and Yarom, 1998; Vos et al., 1999).

An alternative possibility is that axon–oligodendrocyte interactions are disrupted in the mutant mice. Contactin has been localized on oligodendrocytes (Koch et al., 1997) and may promote interactions with axons during myelinogenesis. Consistent with this possibility, focal swellings of Purkinje cell axons have been observed in myelin-deficient mutants such as *jimpy* (Rosenfeld and Freidrich, 1983), *quaking*, and *shiverer* (Suzuki and Zagoren, 1975; Friedrich, 1980). In addition, initial immunohistochemical staining for myelin basic protein has revealed abnormal myelin profiles in the cerebellar fiber layer of contactin mutant mice (E. O. B. et al., unpublished data). Additional studies in our laboratory are aimed at revealing contactin's role in myelination.

A Model for Contactin Function in the Cerebellum

The defects in cerebellar microorganization resulting from ablation of contactin gene expression are summarized in Figure 8. The current study identifies functions of contactin in four discrete processes. (1) Contactin guides granule cell axon populations into the correct perpendicular orientation; (2) contactin, although not required for the formation of parallel fiber fascicles in situ, contributes to the compaction of axons within fascicles; (3) contactin-mediated interactions are necessary for the expansion of granule cell dendritic claws; and (4) contactin regulates the extension of Golgi cell dendrites

into the ML. The combination of these defects may severely compromise neuronal activity in the cerebellum and contribute to the ataxic phenotype. The following model is designed to explain how ablation of contactin-mediated interactions could affect cerebellar activity.

The dendritic fields of granule cells are significantly reduced in the mutant mice. Therefore, postsynaptic area available for afferent mossy fiber and Golgi cell connections is significantly diminished versus that of wild-type mice. During development, an individual granule cell dendritic claw establishes five to six synapses on mossy fibers. For granule cell activation, two granule cell dendrites (with 10–12 synapses) need to be simultaneously activated by a mossy fiber to fire (Hámori and Szentágothai, 1966; Jakab, 1989; D'Angelo et al., 1995). With the reduced granule cell postsynaptic area in contactin mutants, fewer mossy fiber synapses may be formed, and granule cell activation by mossy fibers may be more difficult to achieve. Moreover, misoriented parallel fibers in the outer ML and decreased axon–axon interactions may compromise electrical activity of parallel fiber arrays in contactin mutant mice (Cohen and Yarom, 1998; Vos et al., 1999).

In addition, Golgi cells play an important role in regulating granule cell activity by exerting feedback inhibition on their afferent granule neurons (Eccles et al., 1964), which synchronizes granule cell firing (Maex et al., 1998; Vos et al., 1999). In view of those results, the significant reduction of Golgi cell dendritic fields in mutant mice may attenuate synaptic inhibition at Golgi-granule synapses and yield unsynchronized and abnormal activity of excitatory parallel fibers. Eliminating the function of Golgi cells, as elegantly shown by toxin-mediated cell ablation in transgenic mice, disrupts the Golgi-granule cell feedback loop and affects cerebellar activity (Watanabe et al., 1998). Interestingly, ablation of Golgi cell function alone suffices to generate an ataxic phenotype. In contactin mutants, disrupted Golgi–granule cell interactions may thus affect the synchronized activity of parallel fibers converging on Purkinje cells and compromise the overall output activity of the cerebellar cortex.

In conclusion, our analyses point to a critical role of contactin-mediated interactions in guiding populations of granule cell axons and in supporting dendritic growth of interneuron subpopulations in the cerebellum. The specific nature of these interactions, their interrelations, and the molecular mechanisms underlying contactin function will require more extensive investigation. The contactin mutant mice provide an excellent tool for gaining a deeper understanding of adhesion/recognition events that underlie the formation of the remarkable circuitry responsible for the coordination of motor functions.

Experimental Procedures

cDNA Cloning and Production of Fusion Proteins

A 281 bp cDNA fragment corresponding to the 5′ end of mouse contactin/F3 (Gennarini et al., 1989) was amplified by PCR from a newborn mouse brain cDNA library (Stratagene) and used to isolate full-length cDNA from the same library. Partial sequencing and restriction site mapping confirmed that the isolated cDNA clone was identical to F3 (the mouse homolog of chicken and human contactin; Ranscht, 1988; Berglund and Ranscht, 1994; Reid et al., 1994).

Generation of New Contactin Antisera

Contactin Ig Domain Antiserum

DNA encoding contactin Ig domains (mCNTN-Ig1-6) was amplified by PCR with the forward primer placed 5′ of the signal peptide and the reverse primer (which included a 6× Histidine tag) corresponding to the carboxyl terminus of the Ig domains. The amplified DNA fragment was cloned into the pCEP4-vector (Invitrogen) and transfected into 293 EBNA cells (Invitrogen) by calcium-phosphate precipitation (Pharmacia Biotech). The fusion protein was harvested from serum-free DMEM culture medium and purified on a 1 ml Ni^{2+} column (Qiagen). A rabbit was immunized and boosted with 200 μg mCNTN-Ig1-6 protein at 4 week intervals. For affinity purification, antiserum was absorbed on recombinant contactin protein coupled to cyanogen bromide-activated Sepharose 4B (Pharmacia Biotech). Antibodies were eluted with 100 mM glycine, neutralized with 1 M Tris-HCl (pH 8.0), and dialyzed against phosphate-buffered saline (PBS). Affinity-purified contactin antibodies were specific for the 135 kDa contactin protein in Western blot and immunoprecipitation experiments.

Contactin FNIII Repeat Antiserum

Fusion protein comprising contactin FNIII repeats (mCNTN-FNIII) was generated by cloning corresponding PCR-amplified DNA in frame with glutathione-S-transferase (GST) into the pGEX2T plasmid vector (Pharmacia Biotech). The forward primer was placed 3′ of the hinge region, and the reverse primer corresponded to sequences surrounding the conserved tyrosine in FNIII domain 4. The plasmid was transformed into protease-deficient bacterial cells (TG-1), and fusion protein was generated as described by the manufacturer (Pharmacia Biotech). A rabbit was immunized and boosted with 200 μg of mCNTN-FNIII protein immobilized to the beads at 4 week intervals.

Western Blot Analysis

Equal amounts of soluble protein from cultured neurons or brain tissue from wild-type and mutant mice were subjected to Western blotting (Towbin et al., 1979) with antibodies to mCNTN-Ig1-6, mCNTN-FNIII, chick contactin (Ranscht, 1988), mouse F3 (Gennarini et al., 1989), or rat L1 (Stallcup et al., 1985).

Contactin Targeting Vector and Derivation of Contactin-Deficient Mice

Genomic DNA containing exon 3 and exon 4 (Buttiglione et al., 1995) was isolated from a 129SVJ mouse genomic library (1×10^6 independent plaques; Stratagene) and used to generate the gene-targeting vector. Exon 3, which encodes contactin amino acids 32 to 76 and includes the amino-terminal cysteine (amino acid 65), was disrupted by insertion of a neomycin-resistance cassette (*PGK-neo*; Soriano, 1995) into a mutated XhoI site. Herpes simplex virus thymidine kinase cDNA ([HSV-TK]; Mansour et al., 1988) was added to the 3′ end of the construct as a negative selectable marker (Figure 2B).

The linearized contactin gene targeting vector was electroporated into R1 embryonic stem cells (from Dr. Nagy, Mt. Sinai Hospital, Toronto, Canada; Nagy et al., 1993). A total of 124 double-resistant colonies were tested by Southern blot (Berglund and Ranscht, 1994) or PCR analysis (positions of Southern probe and PCR primers 1, 2, and 3 are indicated in Figure 2A). Three clones were injected into mouse blastocysts of C57Bl/6 females and reimplanted into CD1 pseudopregnant females. Eleven chimeric founder males (eight from one ES cell clone and three from the second clone) carried the mutation in the germline. Mice homozygous for the mutant allele were derived from founders of both lines and had an identical phenotype. Both lines were maintained as a mixed strain (129SVJ × C57Bl/6 × Black Swiss) for the current analyses. In all experiments described in this paper, homozygous mutants were compared with wild-type littermates.

Primary Culture of Cerebellar Neurons

Cerebellar granule cell reaggregate cultures were prepared as described by Gao et al. (1995). The cell suspension was plated onto 0.0005% poly-L-lysine (Sigma) and grown for 72 hr. For antibody-mediated defasciculation studies, anti-mCNTN-Ig1-6 IgGs were used at a concentration range of 0.01 mg/ml-2 mg/ml.

Biotinylation Assay

For cell surface biotinylation, cerebellar granule cell cultures were grown for 48 hr on 35 mm tissue culture dishes coated with 10 μg/ml of poly-L-lysine. Biotinylation was performed as described by Rodriguez-Boulan et al. (1989). Immunoprecipitation with Avidin-Sepharose beads was performed on cell lysates as described by Wollner et al. (1992). Samples were analyzed by Western blotting with anti-mCNTN-Ig1-6 and anti-L1 antisera (courtesy of Dr. W. Stallcup). In reverse experiments, contactin was immunoprecipitated with anti-mCNTN-Ig1-6 antiserum and probed on Western blots with horseradish peroxidase-conjugated avidin. Identical results were obtained in both sets of experiments.

Immunohistochemistry

Three or more littermate pairs of wild-type and mutant mice were used in each experiment. Mice were anesthetized with Avertin (Aldrich) and transcardially perfused with a vascular rinse of 0.9% NaCl followed by 4% formaldehyde in 0.1 M phosphate buffer. Brains were dissected and cryoprotected in 25% sucrose in 0.1 M phosphate buffer overnight at 4°C. After embedding in O. C. T. compound (Sakura Finetek), brains were cryosectioned at 15 μm and collected in PBS.

For immunohistochemistry, tissue sections were washed in Tris-buffered saline (TBS), treated with 0.3% H_20_2 (to block endogenous peroxidase activity), and blocked in a solution of 3% goat serum (Sternberger Monoclonals) and 0.25% Triton X-100 (TX-100; Sigma) in TBS. Sections were then incubated at 4°C for 24–48 hr in primary antibodies diluted in 1% goat serum/0.25% TX-100 in TBS. The following antibodies were used: anti-mCNTN-Ig1-6 at 1:500–1:1000, anti-calbindin D-28 (Swant) at 1:1000, monoclonal antibodies against mGluR2/3 (Chemicon) at 1:1000, and MAP2 at 1:100 (Dr. L. Binder, Northwestern University, Chicago, IL). Sections were washed for 1 hr at room temperature in 1% goat serum/0.25% TX-100/TBS before application of biotinylated secondary antibodies (Vector). Sections were washed in TBS, incubated with ABC tertiary complex (Vector), and washed in TBS. After development in DAB substrate solution (0.05% DAB, 0.01% H_20_2 in Tris), sections were mounted and analyzed with a Nikon Eclipse TE300 microscope.

Standard Electron Microscopy

Preparations for standard electron microscopy were as described (Friedrich and Mugnaini, 1981). The desired cerebellar folia were cut from the sections with a razor and reembedded onto the surfaces of resin blocks, thus retaining the sagittal orientation of the cerebellum. Ultrathin sections were collected on 200 mesh grids and photographed with a Hitachi 600 or a Zeiss EM10 electron microscope.

Quantification of Parallel Fiber Fasciculation

Thin midsagittal sections of midvermal cerebellar folia V and VI were examined in three sets of mutant and wild-type pairs of mice. Electron micrographs were taken from the center of the ML at 20,000× magnification and photographically enlarged to 50,000×. Over 30 fields within astrocyte-enclosed fascicles of parallel fibers were examined for each mouse cerebellum. A field was defined as contiguous parallel fibers that excluded preterminal axons, Purkinje cell dendrites and spines, astrocytic processes, and capillaries. The areas of individual parallel fiber profiles within fields of a contiguous group of parallel fiber fascicles were measured with NIH Image, totaled, and compared to the total field area occupied by the group. Parallel fibers were recognized by their orientation (predominantly orthogonal to the sagittal section plane), the presence of microtubules, occasional mitochondria, and smooth ER. Parallel fiber fasciculation was expressed as the percentage of axon area occupying the field. Fasciculation values obtained from wild-type mice were compared to those from mutant littermates by an unpaired, 2-tailed t test.

DiI Labeling

Pairs of mutant and wild-type littermate mice were perfused with 4% buffered formaldehyde and dissected as described above. DiI (Molecular Probes) was dissolved in 95% dimethylformamide and injected into the ML of the cerebellum for labeling of granule cells. The tissue was kept for 4 weeks in 4% formaldehyde at 30°C. Brains were Vibratome sectioned at 50 μm in the sagittal plane and sections mounted on glass slides. DiI-labeled parallel fibers and single granule cells and their dendrites were visualized by confocal microscopy on a BioRad MRC1024. Areas occupied by single terminal dendritic extensions were measured in wild-type and mutant mice (Metamorph Imaging System; Universal Imaging Corporation; n = 180 wild-type and n = 182 mutants; three animals/group) and analyzed by an unpaired, 2-tailed t test.

To label Purkinje Cells, DiI crystals were placed in the center of the white matter of 1–1.5 mm thick sagittal cerebellar slabs from wild-type and mutants. After incubation for 2 to 4 weeks as above, slices were Vibratome sectioned at 25 to 50 μm and mounted for confocal analysis.

Quantification of mGluR2/3-Positive Golgi Cell Dendritic Projections

Golgi cell dendrites were identified as darkly stained mGluR2/3-positive fibers projecting through the Purkinje cell layer (mGluR2/3 negative) into the ML of the cerebellum. The criterion for inclusion in the statistical analysis was that the apical Golgi cell dendrite fully extended across the Purkinje cell layer and into at least one quarter of the ML. Whole sections taken from midsagittal levels of cerebellum were quantified by counting crossing fibers along the entire length of the Purkinje cell layer from lobules I–X (n = 15 wild-type sections and n = 14 sections from mutants; each from three animals/group). The entire Purkinje cell layer length (from lobules I-X) was measured using NIH Image. The total number of crossing fibers per section was then divided by the total length of the Purkinje cell layer in the section to yield the number of Golgi cell apical stalks crossing the Purkinje cell layer per unit length of Purkinje cell layer. This calculation was performed to correct for size differences in the cerebellum between wild-type and mutant mice. Data were statistically evaluated using an unpaired, 2-tailed t test.

Acknowledgments

We thank Carol Mason (Columbia University, New York, NY) for many valuable discussions and Edward Monosov (Burnham Institute) for guidance in confocal microscopy. Mary E. T. Boyle contributed to the discussion of the model. Gianfranco Gennarini (Bari, Italy), William Stallcup (Burnham Institute), and Lester Binder (Northwestern University, Chicago, IL) kindly supplied antibodies to mouse contactin/F3, rat L1, and MAP2, respectively. This work was supported by the National Science Foundation (IBN 9723934 to B. R.), the March of Dimes (FY-0265 to B. R.), and the National Institutes of Health (NS 38297 and initially HD 25938 to B. R.; and NS 09904 to E. M.). E. O. B. was supported by the Swedish Society for Medical Research, the Swedish Medical Association, and the Medical Research Council of Sweden. K. K. M. and L. W. are students of the Graduate Program in Neuroscience at UCSD.

Received July 8, 1999; revised September 13, 1999.

References

Altman, J., and Bayer, S.A. (1997). Development of the Cerebellar System (New York: CRC Press).

Alvarado-Mallart, R.M., and Sotelo, C. (1982). Differentiation of cerebellar anlage heterotopically transplanted to adult rat brain: a light and electron microscopic study. J. Comp. Neurol. *212*, 247–267.

Baptista, C.A., Hatten, M.E., Blazeski, R., and Mason, C.A. (1994). Cell-cell interactions influence survival and differentiation of purified Purkinje cells in vitro. Neuron *12*, 243–260.

Bäurle, J., and Grüsser-Cornehls, U. (1994). Axonal torpedoes in cerebellar Purkinje cells of two normal mouse strains during aging. Acta Neuropathol. *88*, 237–245.

Berglund, E.O., and Ranscht, B. (1994). Molecular cloning and in situ localization of the human contactin gene (CNTN1) on chromosome 12q11-q12. Genomics *21*, 571–582.

Berglund, E., Thornell, L.E., and Stigbrand, T. (1991). Intracerebral distribution of Gp135, a new human brain glycoprotein. Brain Res. *549*, 292–296.

Brümmendorf, T., and Rathjen, F.G. (1995). Cell adhesion molecules 1: immunoglobulin superfamily. Protein Profile *2*, 980–992.

Brümmendorf, T., Wolff, J.M., Frank, R., and Rathjen, F.G. (1989). Neural cell recognition molecule F11: homology with fibronectin type III and immunoglobulin type C domains. Neuron *2*, 1351–1361.

Brümmendorf, T., Hubert, M., Treubert, U., Leuschner, R., Tarnok, A., and Rathjen, F.G. (1993). The axonal recognition molecule F11 is a multifunctional protein: specific domains mediate interactions with Ng-CAM and restrictin. Neuron *10*, 711–727.

Buttiglione, M., Cangiano, G., Goridis, C., and Gennarini, G. (1995). Characterization of the 5′ and promoter regions of the gene encoding the mouse neuronal cell adhesion molecule F3. Mol. Brain Res. *29*, 297–309.

Buttiglione, M., Revest, J.M., Rougon, G., and Faivre-Sarrailh, C. (1996). F3 neuronal adhesion molecule controls outgrowth and fasciculation of cerebellar granule cell neurites: a cell-type-specific effect mediated by the Ig-like domains. Mol. Cell. Neurosci. *8*, 53–69.

Buttiglione, M., Revest, J.M., Pavlou, O., Karagogeos, D., Furley, A., Rougon, G., and Faivre-Sarrailh, C. (1998). A functional interaction between the neuronal adhesion molecules TAG-1 and F3 modulates neurite outgrowth and fasciculation of cerebellar granule cells. J. Neurosci. *18*, 6853–6870.

Chang, S., Rathjen, F.G., and Raper, J.A. (1987). Extension of neurites on axons is impaired by antibodies against specific neural cell surface glycoproteins. J. Cell Biol. *104*, 355–362.

Cohen, D. and Yarom, Y. (1998). Patches of synchronized activity in the cerebellar cortex evoked by mossy-fiber stimulation: questioning the role of parallel fibers. Proc. Natl. Acad. Sci. USA *95*, 15032–15036.

Cohen, N.R., Taylor, J.S., Scott, L.B., Guillery, R.W., Soriano, P., and Furley, A.J. (1998). Errors in corticospinal axon guidance in mice lacking the neural cell adhesion molecule L1. Curr. Biol. *8*, 26–33.

Cohen-Cory, S., Dreyfus, C.F., and Black, I.B. (1991). NGF and excitatory neurotransmitters regulate survival and morphogenesis of cultured cerebellar Purkinje cells. J. Neurosci. *11*, 462–471.

Cremer, H., Chazal, G., Goridis, C., and Represa, A. (1997). NCAM is essential for axonal growth and fasciculation in the hippocampus. Mol. Cell. Neurosci. *8*, 323–335.

D'Angelo, E., De Filippi, G., Rossi, P., and Taglietti, V. (1995). Synaptic excitation of individual rat cerebellar granule cells in situ: evidence for the role of NMDA receptors. J. Physiol. *484*, 397–413.

Dahme, M., Bartsch, U., Martini, R., Anliker, B., Schachner, M., and Mantei, N. (1997). Disruption of the mouse L1 gene leads to malformations of the nervous system. Nat. Genet. *17*, 346–349.

Durbec, P., Gennarini, G., Goridis, C., and Rougon, G. (1992). A soluble form of the F3 neuronal cell adhesion molecule promotes neurite outgrowth. J. Cell Biol. *117*, 877–887.

Eccles, J.C., Llinas, R., and Sasaki, K. (1964). Golgi cell inhibition in the cerebellar cortex. Nature *204*, 1265–1266.

Faivre-Sarrailh, C., Gennarini, G., Goridis, C., and Rougon, G. (1992). F3/F11 cell surface molecule expression in the developing mouse cerebellum is polarized at synaptic sites and within granule cells. J. Neurosci. *12*, 257–267.

Fazeli, A., Dickinson, S.L., Hermiston, M.L., Tighe, R.V., Steen, R.G., Small, C.G., Stoeckli, E.T., Keino-Masu, K., Masu, M., Rayburn, H., et al. (1997). Phenotype of mice lacking functional deleted in colorectal cancer (Dcc) gene. Nature *386*, 796–804.

Friedrich, V.L., Jr. (1980). Neuronal abnormalities in the cerebellum of quaking and shiverer mice. In Neurological Mutations Affecting Myelination, INSERM Symposium No.14, N. Baumann, ed. (Elsevier North-Holland Biomedical Press), pp. 141–146.

Friedrich, V.L., Jr., and Mugnaini, E. (1981). Preparation of neural tissues for electron microscopy. In Neuroanatomical Tract-Tracing Methods, L. Heimer and M.J. Robards, eds. (New York: Plenum Press), pp. 345–375.

Gao, W.Q., Zheng, J.L., and Karihaloo, M. (1995). Neurotrophin-4/5 (NT-4/5) and brain-derived neurotrophic factor (BDNF) act at later stages of cerebellar granule cell differentiation. J. Neurosci. *15*, 2656–2667.

Gennarini, G., Cibelli, G., Rougon, G., Mattei, M.G., and Goridis, C. (1989). The mouse neuronal cell surface protein F3: a phosphatidylinositol-anchored member of the immunoglobulin superfamily related to chicken contactin. J. Cell Biol. *109*, 775–788.

Gennarini, G., Durbec, P., Boned, A., Rougon, G., and Goridis, C. (1991). Transfected F3/F11 neuronal cell surface protein mediates intercellular adhesion and promotes neurite outgrowth. Neuron *6*, 595–606.

Goodman, C.S., and Shatz, C.J. (1993). Developmental mechanisms that generate precise patterns of neuronal connectivity. Cell *72*, 77–98.

Hámori, J., and Szentágothai, J. (1966). Participation of Golgi neuron processes in the cerebellar glomeruli: an electron microscope study. Exp. Brain Res. *2*, 35–48.

Heintz, N., Norman, D.J., Gao., W-Q., and Hatten, M.E. (1993). Neurogenetic approaches to mammalian brain development. Genome Analysis Volume 6: Genome Maps and Neurological Disorders (Cold Spring Harbor, NY: Cold Srping Harbor Laboratory Press), pp. 19–44.

Hosoya, H., Shimazaki, K., Kobayashi, S., Takahashi, H., Shirasawa, T., Takenawa, T., and Watanabe, K. (1995). Developmental expression of the neural adhesion molecule F3 in the rat brain. Neurosci. Lett. *186*, 83–86.

Jakab, R.L. (1989). Three-dimensional reconstruction and synaptic architecture of cerebellar glomeruli in the rat. Acta Morphol. Hung. *37*, 11–20.

Koch, T., Brugger, T., Bach, A., Gennarini, G., and Trotter, J. (1997). Expression of the immunoglobulin superfamily cell adhesion molecule F3 by oligodendrocyte-lineage cells. GLIA *19*, 199–212.

Lim, D.J., Erway, L.C., and Clark, D.L. (1978). Vestibular Mechanisms in Health and Disease (London: Academic Press).

Maex, R., and De Sutter, E. (1998). Synchronization of Golgi and granule cell firing in a detailed network model of the cerebellar granule cell layer. J. Neurophysiol. *80*, 2521–2537.

Mansour, S.L., Thomas, K.R., and Capecchi, M.R. (1988). Disruption of the proto-oncogene int-2 in mouse embryo-derived stem cells: a general strategy for targeting mutations to non-selectable genes. Nature *336*, 348–352.

Morales, G., Hubert, M., Brummendorf, T., Treubert, U., Tarnok, A., Schwarz, U., and Rathjen, F.G. (1993). Induction of axonal growth by heterophilic interactions between the cell surface recognition proteins F11 and Nr-CAM/Bravo. Neuron *11*, 1113–1122.

Mugnaini, E. (1972). The histology and cytology of the cerebellar cortex. In The Comparative Anatomy and Histology of the Cerebellum: The Human Cerebellum, Cerebellar Connections, and Cerbellar Cortex, O. Larsell and J. Jansen, eds. (Minneapolis: University of Minnesota Press), pp. 201–251.

Nagy, A., Rossant, J., Nagy, R., Abramow-Newerly, W., and Roder, J.C. (1993). Derivation of completely cell culture-derived mice from early-passage embryonic stem cells. Proc. Natl. Acad. Sci. USA *90*, 8424–8428.

Neki, A., Ohishi, H., Kaneko, T., Shigemoto, R., Nakanishi, S., and Mizuno, N. (1996). Pre- and postsynaptic localization of a metabotropic glutamate receptor, mGluR2, in the rat brain: an immunohistochemical study with a monoclonal antibody. Neurosci. Lett. *202*, 197–200.

Palay, S.L., and Chan-Palay, V. (1974). Cerebellar Cortex: Cytology and Organization (New York: Springer-Verlag), pp. 63–99.

Peles, E., Nativ, M., Campbell, P.L., Sakurai, T., Martinez, R., Lev, S., Clary, D.O., Schilling, J., Barnea, G., and Plowman, G.D. (1995). The carbonic anhydrase domain of receptor tyrosine phosphatase beta is a functional ligand for the axonal cell recognition molecule contactin. Cell *82*, 251–260.

Peles, E., Nativ, M., Lustig, M., Grumet, M., Schilling, J., Martinez, R., Plowman, G.D., and Schlessinger, J. (1997). Identification of a novel contactin-associated transmembrane receptor with multiple domains implicated in protein-protein interactions. EMBO J. *16*, 978–988.

Pellegrino, L.J., and Altman, J. (1979). Effects of differential interference with postnatal cerebellar neurogenesis on motor performance, activity level, and maze learning of rats: a developmental study. J. Comp. Physiol. Psychol. *93*, 1–33.

Pesheva, P., Gennarini, G., Goridis, C., and Schachner, M. (1993). The F3/11 cell adhesion molecule mediates the repulsion of neurons by the extracellular matrix glycoprotein J1–160/180. Neuron *10*, 69–82.

Pierre, K., Rougon, G., Allard, M., Bonhomme, R., Gennarini, G., Poulain, D.A., and Theodosis, D.T. (1998). Regulated expression of the cell adhesion glycoprotein F3 in adult hypothalamic magnocellular neurons. J. Neurosci. *18*, 5333–5343.

Ranscht, B. (1988). Sequence of contactin, a 130-kD glycoprotein concentrated in areas of interneuronal contact, defines a new member of the immunoglobulin supergene family in the nervous system. J. Cell Biol. *107*, 1561–1573.

Ranscht, B., Moss, D.J., and Thomas, C. (1984). A neuronal surface glycoprotein associated with the cytoskeleton. J. Cell Biol. *99*, 1803–1813.

Rathjen, F.G., and Jessell, T.M. (1991). Glycoproteins that regulate the growth and guidance of vertebrate axons: domains and dynamics of the immunoglobulin/fibronectin type III subfamily. In seminars in The Neurosciences (W.B. Sounders Company), pp. 297–307.

Rathjen, F.G., Wolff, J.M., Frank, R., Bonhoeffer, F., and Rutishauser, U. (1987). Membrane glycoproteins involved in neurite fasciculation. J. Cell Biol. *104*, 343–353.

Rathjen, F.G., Wolff, J.M., and Chiquet-Ehrismann, R. (1991). Restrictin: a chick neural extracellular matrix protein involved in cell attachment co-purifies with the cell recognition molecule F11. Development *113*, 151–164.

Reid, R.A., Bronson, D.D., Young, K.M., and Hemperly, J.J. (1994). Identification and characterization of the human cell adhesion molecule contactin. Mol. Brain Res. *21*, 1–8.

Rodriguez-Boulan, E., Salas, P.J., Sargiacomo, M., Lisanti, M., Lebivic, A., Sambuy, Y., Vega-Salas, D., and Graeve, L. (1989). Methods to estimate the polarized distribution of surface antigens in cultured epithelial cells. Methods Cell Biol. *32*, 37–56.

Rosenfeld, J., and Freidrich, V.L., Jr. (1983). Axonal swellings in jimpy mice: does lack of myelin cause neuronal abnormalities? Neuroscience *10*, 959–966.

Sakurai, T., Lustig, M., Nativ, M., Hemperly, J.J., Schlessinger, J., Peles, E., and Grumet, M. (1997). Induction of neurite outgrowth through contactin and Nr-CAM by extracellular regions of glial receptor tyrosine phosphatase beta. J. Cell Biol. *136*, 907–918.

Seki, T., and Rutishauser, U. (1998). Removal of polysialic acid-neural cell adhesion molecule induces aberrant mossy fiber innervation and ectopic synaptogenesis in the hippocampus. J. Neurosci. *18*, 3757–3766.

Sidman, R.L. (1968). Development of interneuronal connections in brains of mutant mice. In Physiological and Biochemical Aspects of Nervous Integration, C.F.D, ed. (Englewood Cliffs, New Jersey: Prentice-Hall), pp. 163–193.

Soriano, P. (1995). Gene targeting in ES cells. Annu. Rev. Neurosci. *18*, 1–18.

Spacek, J. (1989). Dynamics of the Golgi method: a time-lapse study of the early stages of impregnation in single sections. J. Neurocytol. *18*, 27–38.

Stallcup, W.B., Beasley, L.L., and Levine, J.M. (1985). Antibody against nerve growth factor-inducible large external (NILE) glycoprotein labels nerve fiber tracts in the developing rat nervous system. J. Neurosci. *5*, 1090–1101.

Suzuki, K., and Zagoren, J.C. (1975). Focal axonal swelling in cerebellum of quaking mouse: light and electron microscopic studies. Brain Res. *85*, 38–43.

Tessier-Lavigne, M., and Goodman, C.S. (1996). The molecular biology of axon guidance. Science *274*, 1123–1133.

Towbin, H., Staehlin, T., and Gordon, J. (1979). Electrophoretic transfer of proteins from polyacrylamide gels to nitrocellulose sheets: procedure and some applications. Proc. Natl. Acad. Sci. USA *76*, 4340–4354.

Volkmer, H., Zacharias, U., Norenberg, U., and Rathjen, F.G. (1998). Dissection of complex molecular interactions of neurofascin with axonin-1, F11, and tenascin-R, which promote attachment and neurite formation of tectal cells. J. Cell Biol. *142*, 1083–1093.

Vos, B.P., Maex, R., Volny-Luraghi, A., and De Sutter, E. (1999). Parallel fibers synchronize spontaneous activity in cerebellar Golgi cells. J. Neurosci. *19*, RC6 1–5.

Walsh, F.S., and Doherty, P. (1997). Neural cell adhesion molecules of the immunoglobulin superfamily: role in axon growth and guidance. Annu. Rev. Cell Dev. Biol. *13*, 425–456.

Watanabe, D., Inokawa, H., Hashimoto, K., Suzuki, N., Kano, M., Shigemoto, R., Hirano, T., Toyama, K., Kaneko, S., Yokoi, M., et al. (1998). Ablation of cerebellar Golgi cells disrupts synaptic integration involving GABA inhibition and NMDA receptor activation in motor coordination. Cell *95*, 17–27.

Wollner, D.A., Krzeminski, K.A., and Nelson, W.J. (1992). Remodeling the cell surface distribution of membrane proteins during the development of epithelial cell polarity. J. Cell Biol. *116*, 889–899.

Yoshihara, Y., Kawasaki, M., Tamada, A., Nagata, S., Kagamiyama, H., and Mori, K. (1995). Overlapping and differential expression of BIG-2, BIG-1, TAG-1, and F3: four members of an axon-associated cell adhesion molecule subgroup of the immunoglobulin superfamily. J. Neurobiol. *28*, 51–69.

Zisch, A.H., D'Alessandri, L., Ranscht, B., Falchetto, R., Winterhalter, K.H., and Vaughan, L. (1992). Neuronal cell adhesion molecule contactin/F11 binds to tenascin via its immunoglobulin-like domains. J. Cell Biol. *119*, 203–213.